551. 510. 41

A study of atmospheric sodium in twilight

T. I. TOROSHELIDZE

Abastumani Astrophysical Observatory, Georgia, USSR

(*Received 2 September 1969*)

ABSTRACT. The method of reckoning with the screening effect of the atmosphere developed by the present writer has made it possible to obtain a more authentic idea about the luminous layer of atmospheric sodium at heights of 70–120 km. This method has also made it possible to establish new properties of this layer (dependence of the height of the layer maximum on the concentration of sodium atoms in the maximum, etc). These conclusions are based on systematic measurements of twilight sodium emission conducted at the Abastumani Astrophysical Observatory. Processing from definite conceptions about the mechanism of formation of the sodium layer theoretical explanations of the seasonal changes in the height and the seasonal developments in the twilight sodium glow intensities are given.

1. Introduction

Observations of the resonance scattering of sunlight by sodium atoms in twilight make it possible to determine the vertical distribution of sodium in the earth's atmosphere. However, the degree of accuracy achieved in calculations is somewhat limited by the uncertainty arising from the need to take account both the height of the earth's shadow and additional 'screening height'. The latter is the result of decreased excitation aroused by solar radiation as it passes through the lower atmosphere. The decreased excitation is described by transmission function $T(h)$ where h denotes the height of a given sun ray at the point of sunset (Fig. 1).

Ways to improve the method of the vertical distribution of atmospheric sodium have been discussed time and again (Chamberlain 1961, Hunten 1967). One of these consisted in obtaining a more exact $T(h)$ transmission function helping to determine the magnitude of the 'screening height' (Bricard and Kastler 1944, Dufay 1947, Vegard 1956; Rundle, Hunten and Chamberlain 1960; Hunten 1962). Another consisted in improving the processing of the twilight curve, *i.e.*, the dependence of the sodium rate on the shadow height with account of the existing 'screening height' magnitudes (Rundle, Hunten and Chamberlain 1960, Hunten 1960). It is a pity that though a relatively high degree of accuracy was achieved through the elaboration of twilight curves, the uncertainty in the screening factor still rendered inadequate the accuracy of the findings on the distribution of atmospheric sodium. As a result many important features characterising the behaviour of the sodium layer could not be revealed even by systematic observations.

The main drawback of the method for reckoning with the atmospheric screening effect consisted in the fact that actual atmosphere with its gradually changing transparency depending on h was replaced by a opaque screen of a set height h_0(screening height), $T(h)$ being 0·5. It is worth noting that the screening height of sodium emission derived by different authors with the help of different methods vary rather widely as can be seen from Table 1.

It is worth noting that all the above authors regard the derived screening height as constant values.

To determine the screening height more exactly it is proposed that Fesenkov's method (1930) be used. His method is known in literature as the 'twilight beam' method. Subsequently it was further developed by Staude (1936) and Rozenberg (1966) in the twilight theory. An essential point raised here in the problem is that luminous sodium is localised in a thin layer at high altitude, the general twilight beam problem considering the glowing (scattering) medium whose density makes up the monotonic height function.

The present paper describes the method proposed by us for determining the screening height and the results obtained through the use of screening height values derived in making up the vertical profiles of the sodium layer on the basis of a five-year period of twilight observations carried out at the Abastumani Astrophysical Observatory.

2. Method for reckoning the Atmospheric Screening Effect

Let us look into the geometry of the phenomenon of twilight. Let us assume that observations are being carried out from point O in the plane of the solar azimuth at α angle to the horizon 00′ (Fig. 1). Initially, for the sake of simplicity, we shall ignore the refraction of rays in the atmosphere. The height of the earth's shadow at the

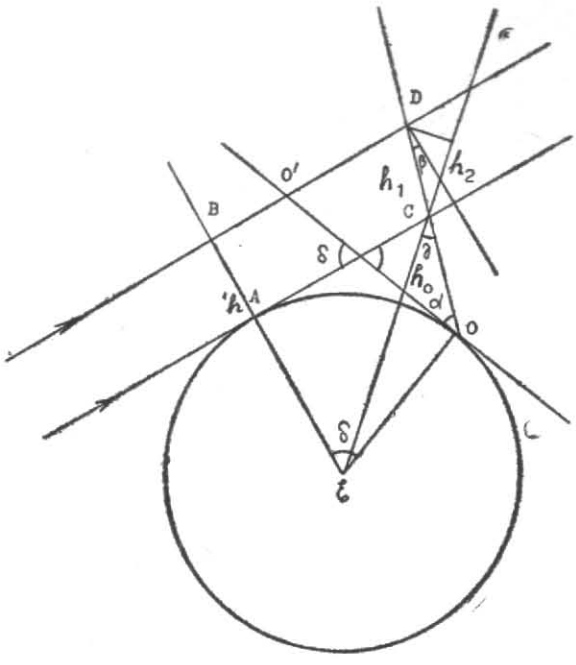

Fig. 1. Simplified model of twilight phenomenon to help determine the effective screening height

point of intersection of a sun ray falling tangentially to the earth's surface and line of sight OD (Point C), the solar depression angle being δ, will be designated H_0; the angle between the normal to the sun ray and the direction of sight (observation), being β; the angle between the direction of scattered light to the observer (*i.e.*, the direction reverse to the direction of observation) and the direction of the vertical line passing through point C being γ. The AB (height h) length projecton on the line of observation will be designated h_1, and in the direction of vertical line at EC is h_2.

Let us also introduce section $H=H_0+h_2$. To calculate the rate of emission of atmospheric sodium in the direction of the observer at a given solar depression angle, it will be necessary to divide section AB$=h$ into elements dh whose projection on the line of observation will be expressed as follows —

$$dh_1 = \frac{dh}{\cos\beta} \qquad (1)$$

Let us represent the concentration of sodium atoms in each dh_1 elementary layer (depending on the height above the earth's surface) in the form of function $\rho_0(H)$ which depends on distance H. The sodium emission rate excited by sunlight in layer dh may be represented as follows—

$$dI = kT(h)\,\rho_0(H)\,dh_1 \qquad (2)$$

where k is the factor of proportionality which depends on sunlight intensity and the fluorescent capacity of sodium. The desired intensity will apparently, be obtained by integration of the latter expression along the line of sight with account of (1)—

$$I(\delta,\alpha) = k\int_0^\infty T(h)\,\rho_0(H)\,\frac{dh}{\cos\beta} \qquad (3)$$

By making use of the geometrical correlations determined by triangles in Fig. 1, we will have —

$$I(\delta,\alpha) = k\,\mu\cos\beta\int_0^\infty T(h)\,\rho_0'(H+\mu h)\,dh_1 \quad (4)$$

where, $\mu = \cos\gamma/\cos\beta$

Under the integral there is a monotonic function $T(h)$ which increases with height h. Its magnitude within 0 and approximately 50-km ranges from zero to one (Rozenberg 1966). The concentration of sodium atoms is zero at heights of $60 \geqslant H_0 + \mu h \leqslant 130$ km (Chamberlain 1961; Hunten 1967). Owing to the essentially positive character of both subintegral functions within the given range of heights there must be a maximum product of these functions for any depression angle δ, which will be proportional to the brightness of sodium emission for any given height $H=H_0+\mu h$. Integral (4) has been calculated numerically by the mechanical quadrature method, by adding the values of subintegral functions every 2, 5 km. The $T(h)$ magnitudes were taken from Bricard and Kastler (1944)

TABLE 1

Sodium emission Screening Heights obtained by different authors

Author	h_0 (km)
Bricard and Kastler (1944)	25
Dufay (1947)	25
Vegard (1948)	40
Hunten (1956)	10
Blamont, Donahue and Weber (1958)	29·5
Rundle, Hunten and Chamberlain (1960)	27·0 (Spring) 26·3 (Autumn)
Hunten (1962)	29·5

and in the case of functions $\rho(H)$ we took advantage of the data of Rundle, Hunten and Chamberlain (1960). The results of the calculations are given in Fig. 2. It can be seen from this figure that the position and the shape of the curves vary with angle δ, its size being shown on the curves. In our calculations we assumed angle α to be 25°. Therefore, for $\delta<6°$, the height $H \leqslant 60$ km. This corresponds to daylight conditions when the observed emission rate could not be opposed to the height of the earth's shadow; for $\delta>14°$ corresponds to night conditions $[J(\delta, \alpha) = 0]$.

For the sake of expedience in comparing the results of our calculations with h_0 "screening height" values used by other authors (Table 1) we would like to introduce the conception of effective screening height, h_{ef}, coined earlier by Staude (1936) for the twilight theory. h_{ef} is the height of the centre of gravity of the luminous layer, *i.e.*, the height of a certain point of the line of sight which corresponds to the effective values of the product of functions $T(h)$ and $\rho_0'(H_0 + \mu h)$—

$$h_{ef} = \mu \frac{\int_0^\infty T(h)\,\rho_0'(H_0 + \mu h)h.\,dh}{\int_0^\infty T(h)\,\rho_0'(H_0 + \mu h)dh}. \qquad (5)$$

The calculated h_{ef} effective screening height magnitudes for the different δ angles are given in Table 2. The values of subintegral function in equation (5) were summed up for every 2, 5 km interval in height. Column 3 of Table 2 gives the h_{ef} values without account of the sun ray refraction in the atmosphere. Column 4 gives the h_{ef} values calculated with account of sun ray refraction and of sun refractional divergence in keeping with data provided by Rozenberg (1966).

TABLE 2

Solar depression angle δ (degrees) (1)	Height of earth's shadow (km) (2)	Effective screening height (h_{ef}) (km) (3)	(4)	(5)	(6)
6	31	38·0	38·8	38·8	34·1
7	37	35·5	35·8	36·4	33·7
8	50	33·0	33·5	33·7	32·0
9	62	28·8	29·5	29·1	30·4
10	74	24·5	25·5	24·5	26·0
11	87	19·2	20·0	20·2	16·2
12	100	14·0	15·7	16·0	13·2
13	112	8·7	12·0	10·9	10·8

It is seen from comparing the figures quoted in Cols. 3 and 4 reckoning the effect of refraction and refractional divergence in calculating the effective screening height introduces but a small increase in the h_{ef} magnitudes. It is worth noting that with an increase in the solar depression angle the difference between the values given in Cols. 3 and 4 tends to grow. This is due to the fact that with an increasing solar depression angle it is necessary in expression (5) to make use of function $T(h)$ for low h heights for which refractional distortion is considerable.

To ascertain the 'stability' of the solution arrived at (5) we calculated the h_{ef} values for other types of $T(h)$ functions in keeping with data given by Blamont, Donahue and Stull (1958) and also for function $\rho(H)$ which differs appreciably from the distribution used in previous calculations. The calculation results are given in Cols. 5 and 6 of Table 2 respectively. By comparing them with the figures given in Cols. 3 and 4 one can see that the choice of the type of transmission function hardly affects the results of calculated h_{ef} values. The effect of function $\rho(H)$ on the magnitude of h_{ef} is somewhat greater than that of function $T(h)$. But in this case too the character of the change in h_{ef} values with a change in the δ angle remains the same. This is indicative of the 'stability' of the solution (5).

The fact that until now there was no strictly established method for calculating the h_0 'screening height' resulted in a wide range of h_0 values arrived at by different authors (*see* Table 1). We can claim now that the figures quoted in Table 2 bring certainty in respect to this problem.

The regular character of the decrease in h_{ef} values with an increase in the solar depression

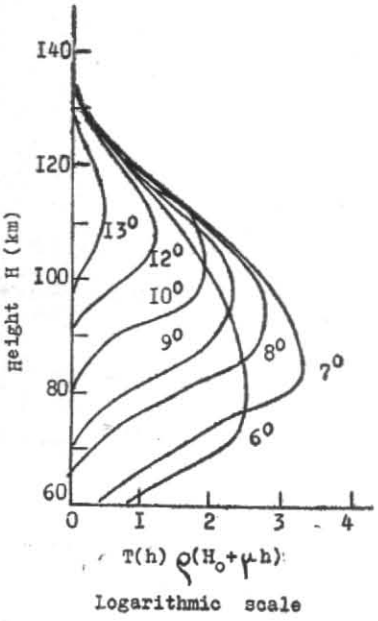

Fig. 2. Twilight layer height models for various solar depression angles (figures close to curves)

Observations being conducted in solar azimuth at an angle 25° to the horizon. Models calculated on the basis of Eq. 4.

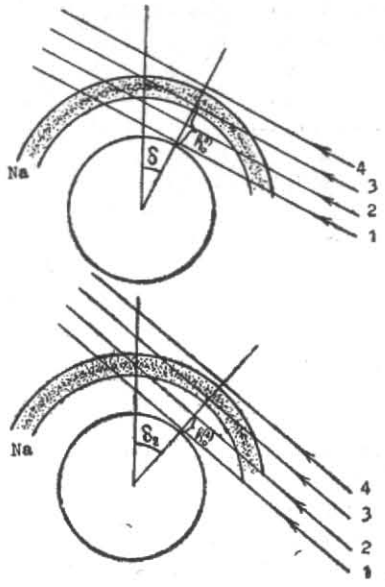

Fig. 3. Apropos of interpretation of h_{ef} effective screening height values (Table 2)

angle within a range of 40 to 10 km shows that the previous assumptions about the screening height being constant are unsound. The change in the h_{ef} values is conditioned by the character of the vertical distribution of the luminous substance: by the presence of sodium atoms in a relatively thin layer at a height of 60-120 km. Indeed, let us conceive an elementary model of twilight for two solar depression moments (Fig. 3) with zenith observation (angles δ_1 and δ_2 where $\delta_2 > \delta_1$). Let us consider a case with several sun rays crossing the line of sight at various distances from the earth's surface (ray 1, 2, 3 and 4). In the case of angle δ_1 ray 3 will most effectively excite sodium atoms, because it illuminates the most dense region of the sodium layer, although it is attenuated to a greater degree than ray 4 as it passes through the bottom layer of the earth's atmosphere. In this case the effective screening height will be h_0^1. As angle δ increases (case 2, Fig. 3) ray 2 will turn out to be the most effective one, for at this moment it will be illuminating the densest region of the sodium layer, although it will be attenuated to a greater degree than rays 3 and 4. In this case the effective screening height will be h_0^2. Obviously $h_0^1 > h_0^2$. With a further increase in angle the effective screening height will continue to decrease until the ray which drops tangentially on the earth's surface (ray 1, Fig. 3) ceases to illuminate the sodium layer, *i.e.*, when twilight is over for the sodium layer.

To find the vertical distribution of sodium in keeping with the data of twilight observations it will be necessary in the first place to determine the layer profile in zero approximation. This can be done by differentiating the twilight curve according to the height assuming that $h_0 =$ constants and by using it on the basis of formula (5) to determine the h_{ef} effective screening height values. We shall then use the obtained h_{ef} values to build in a similar way a new distribution model in the first approximation—$\rho(H)$. It should be pointed out that there is no practical need for calculating the next approximation, for our computations show that it differs only slightly from the curve of the first approximation. It reveals ready convergence in the process of calculating h_{ef} values with the help of formula (5).

It is worth noting that the method for determining the effective screening height, described herein, may be used in the case of other twilight emissions too, as long as resonance scattering forms the mechanism of excitement similar to that of sodium emission.

3. Sodium layer properties in the earth's atmosphere by Twilight Observations

The method described in the previous section has been used for processing a wealth of spectrographic material obtained during twilight observations of atmospheric sodium. These observations were car-

ried out at the Abastumani Astrophysical Observatory in the 1962-1966 period (Megrelishvili and Toroshelidze 1965). Let us consider, for instance, the data on the vertical distribution of sodium atoms which were calculated with the help of our method, *i.e.*, the curves obtained in November (maximum emission of twilight sodium) (Fig. 4) and in June (minimum emission) (Fig. 5). Both graphs show initial twilight curves built in zero approximation (curves marked with letter 'a'). The replacement of constant values (Table 1) by effective screening height magnitudes has caused maximum change (compression) in the twilight curve to occur in the region of δ depression angles being 8-10° (H=82—99 km) with observations being conducted in the solar azimuth at an angle of 25° to the horizon. This "compression" will help to bring about the maximum in differentiating the initial curve (curves 'a' and 'b' in Figs. 4 and 5). However, on the other hand, the maximum position will be determined by the type of the initial twilight curve which, as can be seen from a comparison of curves 'a' in Figs. 4 and 5 is different from November and July. Therefore, the true maximum position will be determined by the sum of both factors.

By comparing the models of vertical distribution obtained in zero approximation for November and July observations we will see that the height of the sodium layer maximum (H_{max}) is approximately at the same level (≈ 80 km). The h_{ef} effective screening heights (first approximation curves) caused different changes in the initial twilight curves for November and July. The November values (Fig. 4) are characterised by a greater intensity inversion in the initial curve (points 1, 2 and 3). The inversion has proved greater than the 'compression' referred to above (curve in the region of points 4, 5 and 6). As a result the maximum in the first approximation has remained at the original level (points 1′, 2′ and 3′ on the curve shown in Fig. 4). In the case of the July curve (Fig. 5) the 'compression' complicated by the 'warping' (points 4, 5 and 6) of initial curve 'a' has determined a new position for the maximum at a level in the region of points 4,′ 5′ and 6′ (curve b). Here the H_{max} value is about 98 km. Thus, the effective screening height values in the case of these two observations have helped to establish that during maximum twilight glow of sodium in November the maximum sodium layer height is approximately 15 km below the summer level (Fig. 5). In addition to this, a comparison of the vertical distribution curves in the first and zero approximation shows the sodium layer to be thinner and sodium atom concentration in the maximum to be higher in the new model.

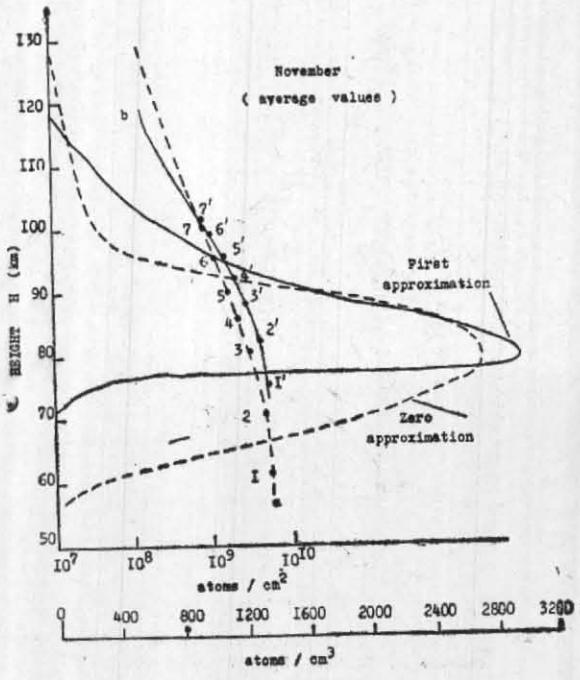

Fig. 4. November (Max. emission)

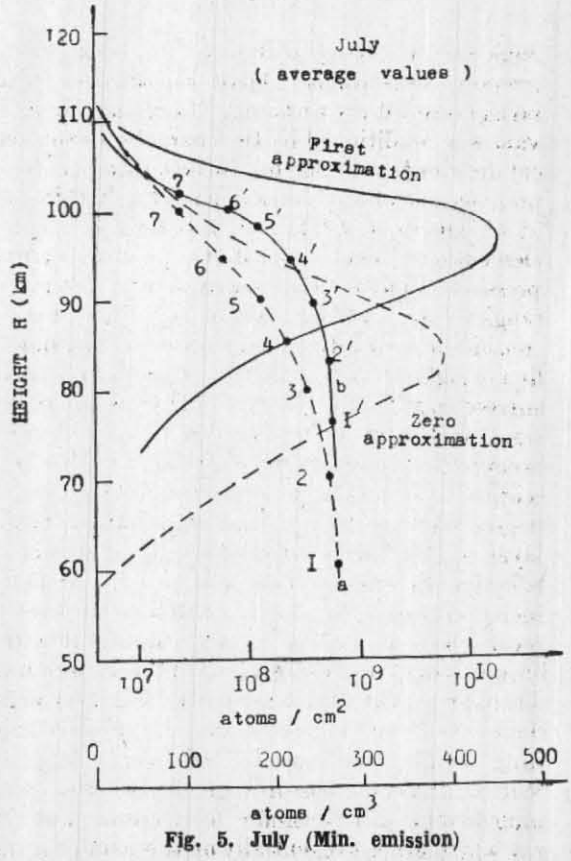

Fig. 5. July (Min. emission)

Figs. 4 & 5. Results obtained from models of vertical distribution of atmospheric sodium in zero and first approximations with corresponding initial twilight curves

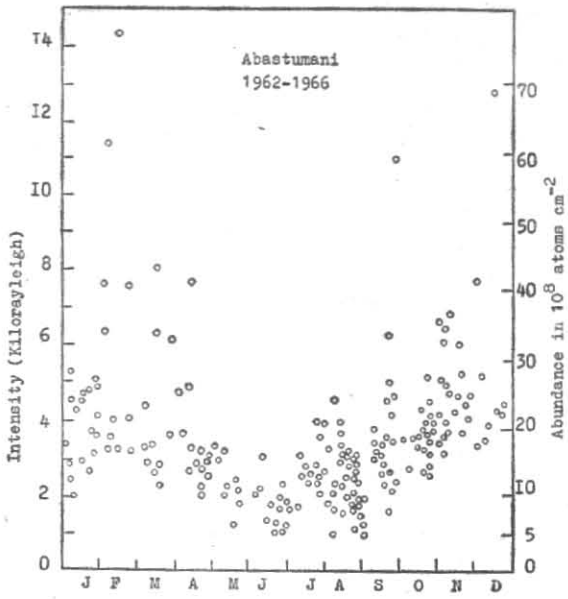

Fig. 6. Seasonal variations in sodium on the basis of separate observations

Similar models built for all the observation materials have confirmed the results following from the above observations. They have made it possible to investigate the peculiarities and regularities that characterise the behaviour of luminous atmosphere sodium. In particular it has been established that—

(*a*) Sodium atom abundance over Abastumani varies between $0{\cdot}8\times10^9$ and 5×10^9 atoms per sq. cm. In summer the abundance of sodium is invariably smaller (by half or even a quarter on the average) that in winter (Fig. 6) ;

(*b*) Sodium concentration (ρ_{max}) in the maximum of the layer may vary from 2000 atoms per cu. cm. (November-December) to 250-300 atoms per cu. cm. in July ;

(c) The half-thickness of the sodium layer makes up about 25 km (in winter it is less);

(*d*) The average H_{max} height of sodium layer maximum in keeping with the first approximation data is greater by 6 km as compared to the figures of zero approximation: 93 km instead of 87 ;

(*e*) The height of the sodium layer maximum depends on the concentration of sodium atoms in the maximum: the higher the concentration, the lower the height (Fig. 7); and

(*f*) In winter the height of the sodium layer maximum H_{max} is lower than in summer (light and dark circles in Fig. 7), the difference being about 10-15 km.

4. Processes occurring in the atmosphere and sodium layer properties

It is possible to make an attempt to explain the above properties of atmospheric sodium, proceeding from the prevailing ideas about the mechanism of formation of the sodium layer. Assuming that according to Chapman (1939) the concentration of atomic sodium in the atmosphere is determined by reduction and oxidation reactions —

$$NaO + O \rightarrow O_2 + Na \qquad (K_1) \qquad (6)$$

$$Na + O_3 \rightarrow NaO + O_2 \qquad (K_2) \qquad (7)$$

Where K_1 and K_2 are rate factors characterising the corresponding reactions, it is possible to obtain a condition of photochemical balance for the sodium layer ;

$$\frac{n(Na)}{n(NaO)} = \frac{K_1 n(O)}{K_2 n(O_3)} \qquad (8)$$

where n ( ) denotes concentrations of atmospheric components.

Assuming that in the atmosphere sodium is distributed according to the exponential law—

$$n(Na) + n(NaO) = n_0 e^{-H/7{\cdot}5} \qquad (9)$$

where H is the height in km and n_0 is concentration of the entire quantity of sodium—both

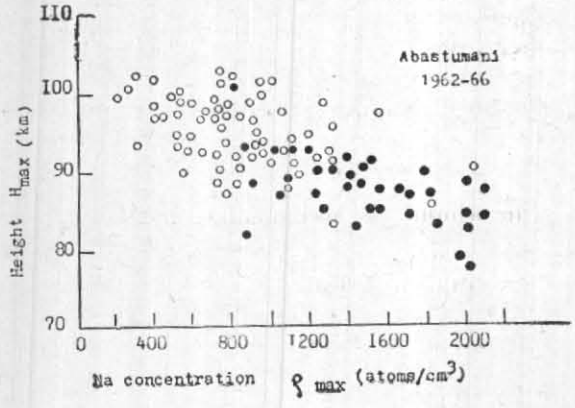

Fig. 7. Dependence of height of sodium layer maximum on the concentration of sodium atoms in the maximum

Data obtained on the basis of observations conducted in the 1962-1966 period at Abastumani (light circles denote summer observations and dark circles winter observations)

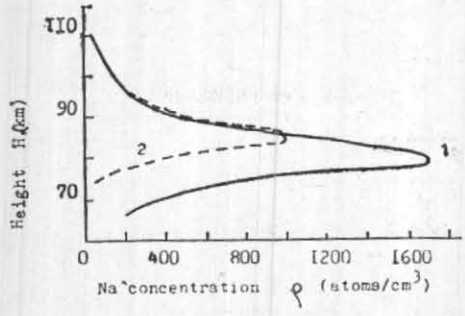

Fig. 8. Vertical distribution of atomic sodium calculated on the basis of formula (10)

Curve 1 corresponds to O and O_3 concentrations for winter values and curve 2 for summer values (Hunt 1966, Khvostikov 1963)

bound and free—Hunten (1954) on the basis of expressions (8) and (9) obtained a relationship for calculating the vertical distribution of atomic sodium in the atmosphere :

$$n(\mathrm{Na}) = n_0 e^{-H^{1.5}} / [1 + K_2 n(\mathrm{O_3}) / K_1 n(\mathrm{O})] \quad (10)$$

Formula (10) shows that value n (Na) at various heights H depends on the $n(O_3)/n(O)$ relation which as is known (Khvostikov 1963) can vary widely at heights we are interested in depending on the intensity of one atmospheric process or another. In keeping with Kellogg's estimates (1961) the lower thermosphere of the medium and high latitudes is prevailed by ascending in summer and by descending motions in winter. These motions should be accompanied by an appreciable change in the $n(O)$ values at the above heights: in the case of descending motion n (O) should show a marked increase, whereas in the case of ascending motions it should how a drop. Owing to this the seasonal hanges in the sodium layer may be due to the effect of dynamic processes occurring in the higher atmosphere. Indeed, if n (O) increases in winter the H_{max} height should decrease in keeping with formula (8). If n(O) decrease in summer, the H_{max} height should increase. In keeping with formula (10) such a change in n (O) should cause an increase in n (Na) in winter and a decrease in summer which fully conforms to our observations. This effect should be more marked in connection with a seasonal change in $n(O_3)$: an increase in $n(O_3)$ at high altitudes in summer (Paetzold 1955; Rawcliffe and Elliott 1966). Calculation of n(Na) distribution curves in height on the basis of formula (10) has fully confirmed the above : in Fig. 8 curve 1 has been calculated for n(O) and $n(0_3)$ concentrations largely to conform to winter conditions, whereas curve 2 has been calculated to meet summer conditions (Hunt 1966).

5. Conclusion

The method for determining the effective screening height for sun rays, developed by us has made it possible to bring clarity into the

question of the 'screening height'. The calculated h_{ef} values have revealed the regular character of the decrease in the h_{ef} value as the solar depression angle increases with the range of 40-10 km, contrary to the existing opinion about the screening height during twilight being constant. The results obtained can be explained on the basis of elementary ideas about the geometry of phenomena occurring during twilight.

Building models of vertical distribution of atomic sodium with the help of h_{ef} values on the basis of twilight observations conducted at the Abastumani Observatory has made it possible for the first time to establish the seasonal variations in the height of the layer maximum which are characterised by an amplitude offering a sound explanation of the seasonal developments in sodium glow. A theoretical estimate made on the basis of the existing assumptions about the formation of the sodium layer in the atmosphere is in full conformity with the results of the observations : an increase in the height of the layer which is accompanied by a drop in the quantity of sodium in summer is due to a corresponding increase in ozone and a decrease in atomic oxygen in the lower mesosphere in that season. An increase in the quantity of sodium in winter is accompanied by a corresponding decrease in the height of the layer maximum. This occurs as a result of a reverse process: decrease in the abundance of ozone increase in atomic oxygen at heights 60-80 km.

REFERENCES

Blamont, J. E., Donahue, T. M. and Stull, V. R.	1958	*Ann. Geophys.*, **14**, pp. 253-282.
Blamont, J. E., Donahue, T. M. and Weber, W.	1958	*Ibid.*, **14**, pp. 282-304.
Bricard, I. and Kastler, A.	1944	*Ibid.*, **1**, pp. 53-91.
Chamberlain, I. W.	1961	*Physics of the aurora and airglow*, Academic Press, New York & London, Ch. 10.
Chapman, S.	1939	*Astrophys. J.*, **90**, pp. 309-316.
Dufay, J.	1947	*C. R. Acad. Sci., Paris*, **225**, pp. 690-692.
Fessenkov, G. V.	1930	*Astrophys. J.*, **7**, 2 (USSR), pp. 100-112.
Hunt, B. G.	1966	*J. geophys. Res.*, **71**, 5, pp. 1385-1402.
Hunten, D. M.	1954	*J. atmos. terr. Phys.*, **5**, pp. 44-56.
	1956	*Ibid.*, **9**, pp. 179-183.
	1960	*Ibid.*, **17**, pp. 295-301.
	1962	*Ibid.*, **24**, pp. 333-338.
	1967	*Space Sci. Rev.*, **6**, pp. 493-573.
Kellogg, W. W.	1961	*J. Met.*, **18**, 3, pp. 373-381.
Khvostikov, I. A.	1963	*Physics of ozonosphere and ionosphere*, Moscow, Ch. 1, 3.
Megrelishvili, T. G. and Toroshelidze, T. I.	1965	*Bull. abstuman. astrofiz. Obs.*, 32, pp. 165-182.
Paetzold, H. K.	1955	*J. atmos. terr. Phys.*, **7**, pp. 128-140.
Rawcliffe, R. D. and Elliott, D. D.	1966	*J. geophys. Res.*, **71**, pp. 5077-5091.
Rozenberg, G. V.	1966	*Twilight*, Plenum Press, New York, Ch. III, IV.
Rundle, H. N., Hunten, D. M. and Chamberlain, J.W.	1960	*J. atmos. terr. Phys.*, **17**, pp. 205-219.
Staude, N. M.	1936	Publ. of the Comm. for the study of the stratosphere, Acad. Sci. USSR, I.
Vegard, L.	1948	*Nature*, **162**, p. 300.